



OPEN

Isolation and characterization of a *Vibrio owensii* phage phi50-12

Ling-Chun Lin[✉] & Yu-Chuan Tsai

Vibrio owensii is a widely distributed marine vibrio species that causes acute hepatopancreatic necrosis in the larvae of *Panulirus ornatus* and *Penaeus vannamei*, and is also associated with Montipora white syndrome in corals. We characterized *V. owensii* GRA50-12 as a potent pathogen using phenotypic, biochemical, and zebrafish models. A virulent phage, vB_VowP_phi50-12 (phi50-12), belonging to the N4-like *Podoviridae*, was isolated from the same habitat as that of *V. owensii* GRA50-12 and characterized. This phage possesses a unique sequence with no similar hits in the public databases and has a short latent time (30 min), a large burst size (106 PFU/infected cell), and a wide range of pH and temperature stabilities. Moreover, phi50-12 also demonstrated a strong lysis ability against *V. owensii* GRA50-12. SDS-PAGE revealed at least nine structural proteins, four of which were confirmed using LC-MS/MS analysis. The size of the phi50-12 genome was 68,059 bp, with 38.5% G + C content. A total of 101 ORFs were annotated, with 17 ORFs having closely related counterparts in the N4-like vibrio phage. Genomic sequencing confirmed the absence of antibiotic resistance genes or virulence factors. Comparative studies have shown that phi50-12 has a unique genomic arrangement, except for the well-conserved core regions of the N4-like phages. Phylogenetic analysis demonstrated that it belonged to a group of smaller genomes of N4-like vibrio phages. The therapeutic effect in the zebrafish model suggests that phi50-12 could be a potential candidate for application in the treatment of *V. owensii* infection or as a biocontrol agent. However, further research must be carried out to confirm the efficacy of phage50-12.

The genus *Vibrio* comprises a large number of bacterial species that are widespread in coastal oceans¹. In recent years, many new marine *Vibrio* species have been isolated, identified, and analyzed because of their unique physiological and ecological characteristics^{2,3}. Among them, the Harveyi clade, which contains many species related to fishery or coral pathogenicity^{4–8}, has attracted much attention. For example, *Vibrio harveyi* is not only an important pathogenic bacterium that causes fish and crustacean infections, but also is an important research model for studying quorum sensing mechanisms in the cooperative behavior of bacteria⁹. The Harveyi clade in the *Vibrio* group contains five major marine pathogenic bacteria¹⁰, *V. harveyi*, *V. campbellii*, *V. owensii*, *V. jasicida*, and *V. rotiferianus*. They are well-recognized aquatic animal pathogens, but misclassification is common due to similarities in their rRNA sequences and phenotypes^{11,12}.

This study majorly focuses on *V. owensii* which was officially identified and published by Australian microbiologists Leigh Owens in 2010, and the published strain was isolated from diseased shrimp in lobster farms¹³. *V. owensii* is a gram-negative, facultative anaerobic bacterium with a terminal flagellum. It has been recognized as a marine animal pathogen. A previous study reported that *V. owensii* can cause infection of larval cultures in the breeding stock of *Panulirus ornatus*, resulting in serious economic losses¹⁴. A study of Artemia (brine shrimp) mixed with *V. owensii* DY05, used as food for lobster larvae found that the cumulative lethality rate reached 84–89% after 72 h¹⁴. Anatomical analysis of the tissue showed that *V. owensii* was attached to the hepatopancreas and caused necrosis of epithelial cells (Acute hepatopancreatic necrosis disease, AHPND). This showed that *V. owensii* DY05 is a virulent enteric bacterium of *Panulirus ornatus*. However, necrotic infection of the hepatopancreas in lobster seedlings caused by *V. owensii* is not a special case of DY05, and other researchers have isolated a virulent *Vibrio owensii* strain SH-14 as the causative agent of AHPND in cultured shrimp¹⁵. Genome analysis revealed that this strain contained a plasmid. This plasmid was sequenced, analyzed, and found to be similar to the plasmid contained within strain *V. parahaemolyticus*, which has been reported to cause acute hepatopancreatic necrosis disease in the past¹⁶. These plasmids are 99.1% similar and are therefore considered to be associated with acute hepatopancreatic necrosis¹⁷. Studies have also shown that *V. owensii* is associated with Montipora white syndrome in the Hawaiian Islands⁸. Coral bleaching has gained considerable attention in Taiwan recently¹⁸. Previous studies suggest that *V. owensii* can infect aquatic animals, but its toxicity mechanism remains unclear.

Masters Program in Biomedical Sciences, School of Medicine, Tzu Chi University, No. 701, Sec. 3, Zhongyang Rd., Hualien 97004, Taiwan. ✉email: lcl2108@gmail.com

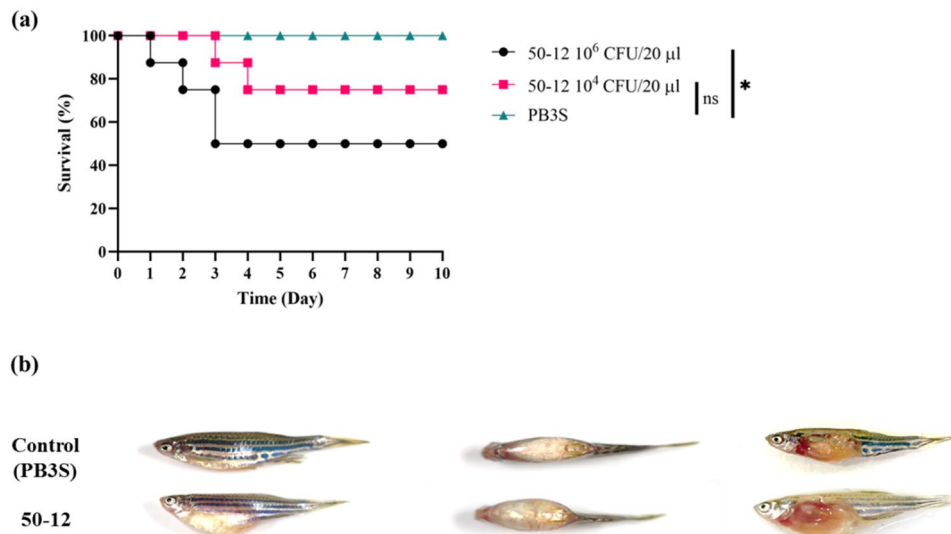


Figure 1. Pathogenicity of *V. owensii* GRA50-12 was confirmed by using zebrafish as a model. **(a)** Three groups (8 fishes/group) were considered, and their survival rates were measured after intraperitoneal injection of *V. owensii* GRA50-12 cells (2.2×10^6 CFU/20 μ l, black line; 2.2×10^4 CFU/20 μ l, red line) or PB3S (PBS with 3% NaCl) as control (green line). The X-axis represents the time post-infection and the Y-axis represents the survival percentage of the zebrafish. **(b)** The disease symptoms in *V. owensii* GRA50-12 infected zebrafish. Control represents PB3S buffer injected fish; thus, no symptoms were observed. 50-12 represents zebrafish injected with GRA50-12 and these showed swollen abdomen and bleeding at body surface (left: side view; middle: top view; right: abdomen anatomy). The anatomical analysis showed swollen and bleeding intestines. The significance of the differences between groups was performed by Log-rank and Gehan–Breslow–Wilcoxon test in GraphPad Prism 9. “*” indicates $p < 0.05$.

Overuse of antibiotics in aquatic farms increases antibiotic resistance¹⁹. Phages have gained attention as biocontrol or therapeutic agents²⁰. To date, only a few phages have been reported against *V. owensii*²¹. In this study, we used *V. owensii* GRA50-12 as the host to isolate and identify phages that can be used to treat *V. owensii* infection.

Results and discussion

Biological characteristics of *V. owensii* GRA50-12. *V. owensii* GRA50-12 was isolated from a coral-associated macroalgae symbiome in the intertidal zone of eastern Taiwan. The whole genome sequence obtained using shotgun sequencing has been published and deposited at DDBJ/EMBL/GenBank under accession numbers BBPJ01000001 to BBPJ01000051. Using Illumina Solexa as the sequencing platform, with 652 \times genome coverage, the current status of this draft genome was noted as “high quality draft”²². According to the Genome Neighbors report provided by NCBI (Supplementary Table S1), the most closely related species are OCN002²³ with 90% sequence identity, strain bablab_jr007²⁴ with 89.8% identical sequence, and one completely sequenced genome XSBZ03²⁵ with 89.5% sequence identity. All of these have been isolated from diseased corals. This suggests that some *V. owensii* shares similar genetic composition in certain ecological niches. When grown on TSB3S routine culture plates, GRA50-12 showed smooth and opaque colonies (Supplementary Fig. S1). Pathogenicity is often attributed to many secretory substances, such as proteases, hemolysins, lipases, or bacteriocin-like substances. Clinical isolates of *V. parahaemolyticus* often produce hemolysins on Wagatsuma agar plates²⁶. Hemolytic activity tests were performed on Wagatsuma agar plates. Our results demonstrated a clear zone surrounding the bacteria (Supplementary Fig. S1), indicating the hemolytic ability of *V. owensii* GRA50-12. This result is similar to that of clinical isolates of *V. parahaemolyticus* which produce heat-stable hemolysin²⁶. The API20E test revealed that GRA50-12 has biochemical characteristics identical to *V. owensii* pathogenic strains DY05 and 47666-1 with the result A-/L+/O+ (Supplementary Table S2)¹⁴. *V. owensii* strain DY05 has been demonstrated to be the etiological agent in larviculture of the ornate spiny lobster (*Panulirus ornatus*), which causes rapid and reproducible larval mortality with pathologies similar to those seen during epizootics.

Zebrafish were used as a model to confirm the pathogenicity of GRA50-12. Several pathogenic *Vibrio* species used in zebrafish models have been previously described, and are highly relevant to real fish models²⁷. When 2×10^6 CFU/20 μ l of GRA50-12 was injected into zebrafish through the cloaca, fish death reached LD₅₀ after 3 days (Fig. 1a). The diseased fish showed distinguished symptoms with a swollen abdomen, and anatomical analysis showed swollen and bleeding intestines (Fig. 1b). These results suggest our zebrafish model showed that GRA50-12 causes fish diseases and the model is useful for demonstrating the effectiveness of phages in controlling the disease.

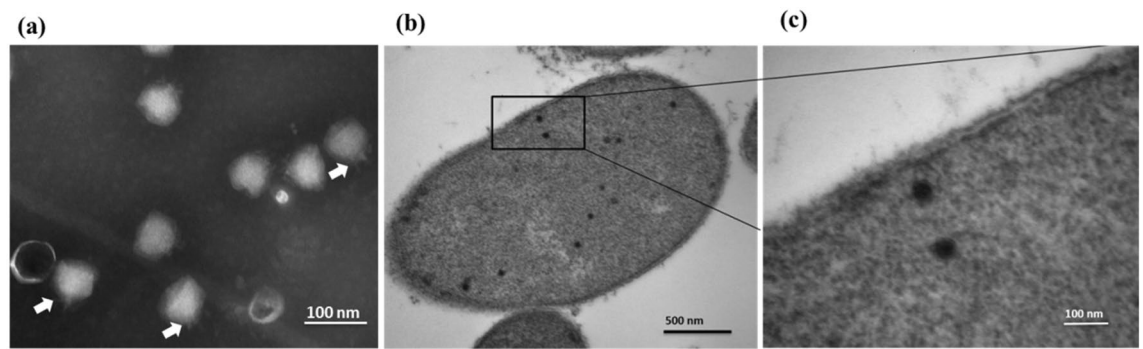


Figure 2. Morphology of phi50-12. (a) Electron micrograph of phi50-12 demonstrates that it resembles podoviruses with short tails; arrow heads indicate the tails of phi50-12. (b) Electron micrograph of thin section reveals phi50-12 virions inside the cell and (c) the loss of cell surface integrity during the release of virions.

Phage morphology and biological properties. *Vibrio* phage phi50-12 was isolated from a water sample from the intertidal zone around the location where the host *V. owensii* GRA50-12 was isolated. The plaques of phi50-12 formed on the lawns of GRA50-12 displayed a halo surrounded by a clear zone which increased in size as time progressed from day 1 to day 3 (Supplementary Fig. S2). This might indicate depolymerase activity, as previously reported²⁸. The isolated phage was designated as phi50-12 based on its host origin. Cesium chloride-purified phage particles were concentrated, and their morphology was examined by TEM (Fig. 2a). Morphologically, phi50-12 showed visibly short tails with icosahedral capsid heads; it resembled podoviruses. The size of the capsid is approximately 70 nm. Electron micrographs of ultrathin sections demonstrated mature phi50-12 virions that were released along the surface of *V. owensii* GRA50-12; at sites where virus particles were released, membrane integrity was lost eventually resulting in cell lysis (Fig. 2b,c, and Supplementary Fig. S3).

The adsorption of phi50-12 reached 60% after 3 min, and no free unadsorbed phages were detected until 21 min post-infection (Supplementary Fig. S4). The latent interval between adsorption and the beginning of the burst was 30 min (Supplementary Fig. S4), and the average burst size was 106 PFU/infected cell. To evaluate the lytic activity of phi50-12, *in vitro* lysis was performed using different multiplicity of infection (MOI). The results indicated that phi50-12 could reduce or inhibit bacterial growth rapidly in the early growth stage, and that this was maintained for at least 10 h at different MOIs applied (Supplementary Fig. S5). Interestingly, with higher MOI, a low frequency of phage-resistant bacteria was generated, which switched their colony morphotype from opaque to translucent (Supplementary Fig. S6). Naturally, many *Vibrio* species display opaque and translucent colony types, such as *V. parahaemolyticus* and *V. alginolyticus*^{29,30}. Colony morphological changes involving physiological, biological, and virulence activity changes have been described^{31,32}. In our study, translucent colony variants showed reduced sensitivity to phi50-12 (data not shown). The opaque and translucent phenotypes of *V. owensii* are plausibly caused by phase variation. A similar observation has been observed with *Bacteroides intestinalis* in a study examining infecting crAss-like phage crAss001³³. However, further investigation is required to verify this hypothesis.

We determined the host ranges by spot tests and confirmed the results using plaque assays with a range of Harveyi-clade *Vibrio* species, including several strains of *V. parahaemolyticus*, *V. alginolyticus*, and *V. harveyi* (Table 1). The results showed that phi50-12 is a host stringent phage, and only *V. owensii* GRA50-12 and *Vibrio* sp. I55-5 (isolated from different types of algae) were infected by phi50-12. I55-5 was sequenced using 16S rRNA sequencing, and was identified as *V. harveyi*. The restricted host range was also observed in phages JA1 and VCO139 infecting *V. cholera*³⁴.

Phi50-12 was subjected to several stresses to simulate environmental conditions. To evaluate the stability of viral particles, we assessed their infectivity at 15 min and 1 h of UV exposure, and at different salt concentrations, temperatures, and pH values for 24 h. The results showed that the particles were very sensitive to UV radiation, but had a high tolerance to salt fluctuation. In addition, phi50-12 showed a wider range of pH stability and lost activity at pH 3 (Fig. 3a). When exposed to various temperatures, the results showed phi50-12 to be stable at 4, 25, 37 °C but lost 18% activity at 60 °C and 100% at 75 °C (Fig. 3b).

Genomic sequence and analysis. The genome size of phi50-12 was estimated to be 65–70 kb according to the results of pulse field gel electrophoresis (PFGE) (Supplementary Fig. S7). The purified phi50-12 DNA showed resistance to frequently used restriction enzymes, including BamHI, KpnI, PstI, SacI, SphI, and XbaI, indicating the existence of potential restriction modification systems. The complete genome sequence of phi50-12 is submitted to GenBank (Accession number MN584918.1), and the accurate genome size is 68,059 bp. The GC content of phi50-12 is 38.5%, which is lower than that of GRA50-12 (45.5%). Nucleotide sequence analysis using BlastN against the nt database revealed no related sequences in the public database. Using BlastP, 101 ORFs were annotated and grouped by functional modules (Fig. 4, Supplementary Table S3). Forty-nine ORFs matched homologs in the available databases, where seventeen of them have closely related counterparts in the N4-like *Vibrio* phage (Supplementary Table S3). Similar to other N4-like phages, the majority of conserved homologs preserve the unique features, such as complete sets of RNA polymerases for orderly transcriptional expression, DNA replication, and capsid formation. No tRNA or tmRNAs were identified in phi50-12 using

Species	Strains	Infectivity	Sources
<i>V. owensii</i>	GRA50-12	+	²²
	051011B	-	Urbanczyk H ^a
<i>V. campbelli</i>	151112c	-	Urbanczyk H
<i>V. hyugaensis</i>	090810a	-	⁶⁰
<i>V. jasicide</i>	090810c	-	⁶¹
<i>V. spp.</i> [*]			
	2-13	-	This study
	8-11	-	This study
	16-10	-	This study
	18-4	-	This study
	55-5	+	This study
<i>V. harveyi</i>			
	BCRC13812 (ATCC25919)	-	BCRC ^b
	0007	-	Chen CY ^c
	0200	-	Chen CY
	2233	-	Chen CY
<i>V. alginolyticus</i> [*]	15-1	-	This study
<i>V. parahaemolyticus</i>	93	-	Yu MS ^c
	10806	-	Yu MS

Table 1. Host range of phi50-12 against *Vibrio* spp. in this study. ^aUniversity of Miyazaki, Miyazaki, Japan; ^bBioresource Collection and Research Center, Taiwan; ^cTzu Chi University, Hualien, Taiwan, ^{*}Identification by selective medium TCBS and 16S rRNA sequencing.

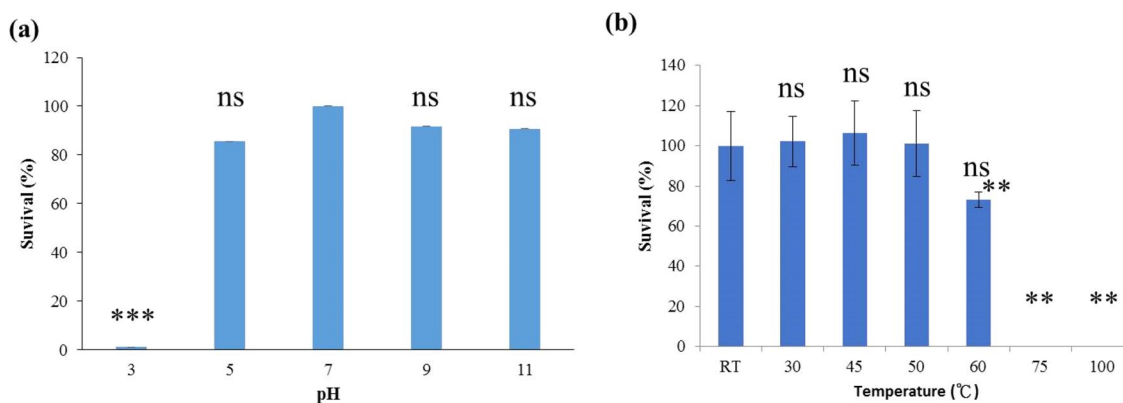


Figure 3. pH and thermal stability of phi50-12. (a) 10^6 PFU of phi50-12 were subjected to various pH at 30 °C for one hour and titrated by plaque assay using a double-layer method; (b) phi50-12 stability (10^6 PFU) under various temperatures for 1 h was measured by plaque assay. The survival rate was measured by comparison with initial phage number. The experiments were performed in triplicates and the data are shown as the mean \pm SEM. Student's *t* test was performed for significance. Ns no significance; ***p* < 0.01; ****p* < 0.001.

Aragorn³⁵ and tRNAScanSE³⁶, and no antibiotic resistance genes or virulence factors were found by ResFinder and VirulenceFinder³⁷.

One of the unique features of N4 particle is the virion-encapsidated RNA polymerase (vRNAP). Genomic analysis of phi50-12 also revealed a large ORF (ORF19) with 3024 amino acids that matched N4 gp50 (vRNAP), which is responsible for early transcription³⁸ and the facilitation of the injection of viral DNA into the host. Although smaller than other vRNAP in N4 and N4-like phages, the result of BlastP showed that phi50-12 vRNAP possesses a conserved domain, and was closely related to the vRNAP gene of *Vibrio* phage VCO139³⁴. Phi50-12 encodes two RNA polymerases (RNAP1 and RNAP2); both of these are subunits of N4 RNA polymerase II; together with gp2 (another subunit), they transcribe the middle genes during the phage life cycle³⁹. However, gp2 homologs were not detected in phi50-12. Many ORFs in phi50-12 have no known functions, and gp2 is likely to be functionally replaced by other ORFs. Similar to the arrangement of *Vibrio* N4-like phages, small insertions (~1.7 kb) between RNAP1 (ORF89) and RNAP2 (ORF84), have also been found in phi50-12³⁴. ORFs

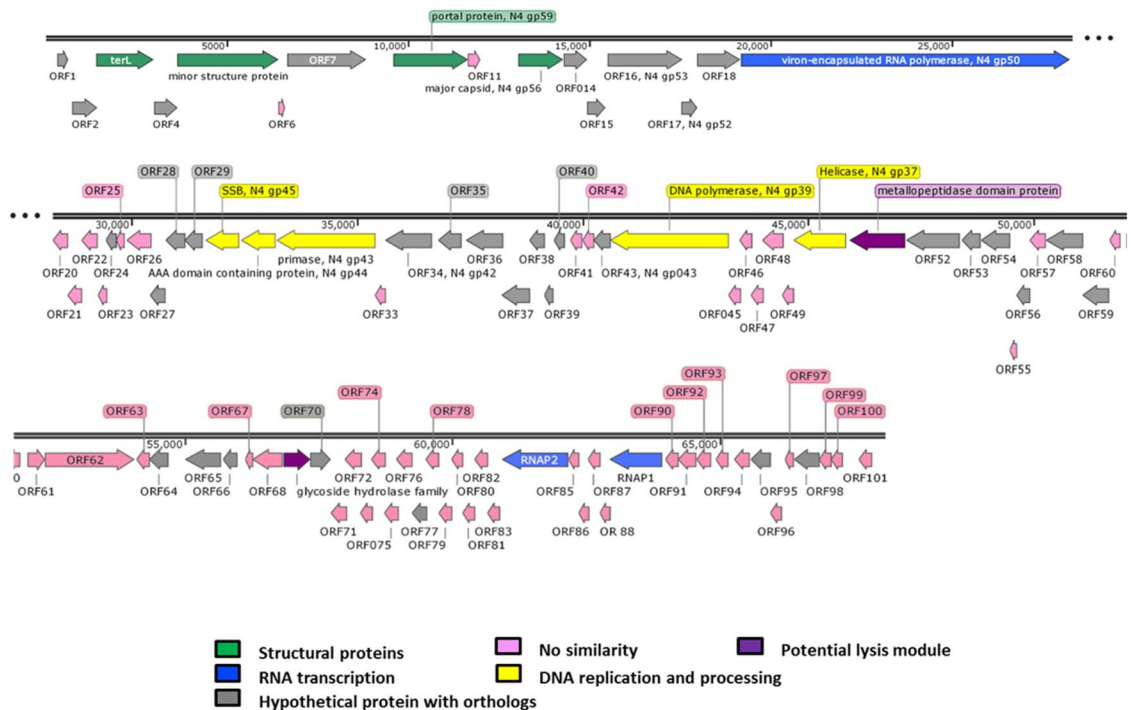


Figure 4. Genomic organization of phi50-12. Direction of the arrow represents transcription orientation. Colored box represents their functionality or uniqueness.

between the two RNA polymerases were predicted to be hypothetical proteins with no similarity hits in the public database. Genes essential for N4 replication, including DNA helicase (ORF50, N4 gp37-like), DNA polymerase (ORF44, N4 gp39-like), primase (ORF32, N4 gp43-like), and single-stranded DNA-binding protein (ORF30, N4 gp45-like) are conserved in the genome. The packaging system components, including the portal protein and the terminase large subunit, were recognized as ORF10 and ORF3, respectively. No lysis cluster could be identified, and only two proteins containing either a metallopeptidase domain (ORF51) or a glycoside hydrolase family protein (ORF69) may be involved in host lysis. In N4-like phages, different groups of lysis clusters with variable gene content have been described previously⁴⁰, such as phage VBP47, and VBP32, which also do not contain any identified lysis cluster. Most lysis clusters of N4-like phages were located upstream of the portal protein but may arrange in different orientations. In the case of *Vibrio* phage VCO139, endolysin is located upstream of RNA polymerase³⁴. The alternative arrangement of lysis clusters made their identification much more difficult.

For better visualization and confirmation, we performed two staining methods to detect the structural proteins in phi50-12. The results showed that at least nine structural proteins of the phi50-12 virions were detected by SDS-PAGE (Fig. 5a,b). The gel band pattern is similar to the protein profiles of JA1 and VCO139, two closely related N4-like vibrio phages of *V. cholerae*³⁴. The results revealed major bands corresponding to the major coat protein (ORF 13), vRNAP (ORF 19), minor structural proteins (ORF7), and portal protein (ORF10) (Fig. 5a,b). LC/MS/MS analysis was performed to confirm the identity of the structural proteins.

One minor structural protein (ORF5) was predicted to be a polysaccharide lyase enzyme due to its similarity with JA1_0065 in JA1. This enzyme is speculated to exhibit substrate specificity³⁴.

Comparative genomics. The nucleotide sequence of phi50-12 did not show any closely related sequences in the public database; however, the annotated ORFs matched some N4-like vibrio phages. Therefore, we performed genomic comparisons using Easyfig and Mauve alignment to demonstrate the conserved part of phi50-12 with N4-like vibrio phages. The results showed that the conserved part of the genomic organization of phi50-12 was located in the core region of genomes of N4-like vibrio phages (genome size smaller than 70 kb) (Fig. 6a) and short fragments of the collinear region of selected N4-like vibrio phages (Fig. 6b). Both results confirmed that phi50-12 is a novel *Vibrio* N4-like phage. All smaller genomes of N4-like vibrio phages, including phi50-12, lack a fragment encoding N4 gp24 and gp25 (rIIA- and rIIB-like proteins); therefore, their genome lengths are shorter than those of other N4-like phages or N4-like vibrio phages. rIIA and rIIB have been reported to be involved in preventing host lysis during phage propagation⁴¹; therefore, the burst sizes of N4 and *Achromobacter* phage phiAxp-3 are relatively large, reaching 3000–9000 PFU/infected cells^{42,43}. In phi50-12, the burst size was 106 PFU/infected cells, much less than the N4 burst size, and electron micrography confirmed that no aggregations of virions were present inside the cell (Fig. 2b,c and Supplementary Fig. S3). Whether or not the lack of rIIA and rIIB fragments influences the burst size needs to be determined in further studies.

Phylogenetic analysis. Due to the increasing number of N4-like members, ICTV has accepted and reclassified the N4 phage and N4-like phages into a new family, *Schitoviridae*, named after Giancarlo Schito⁴⁴. This

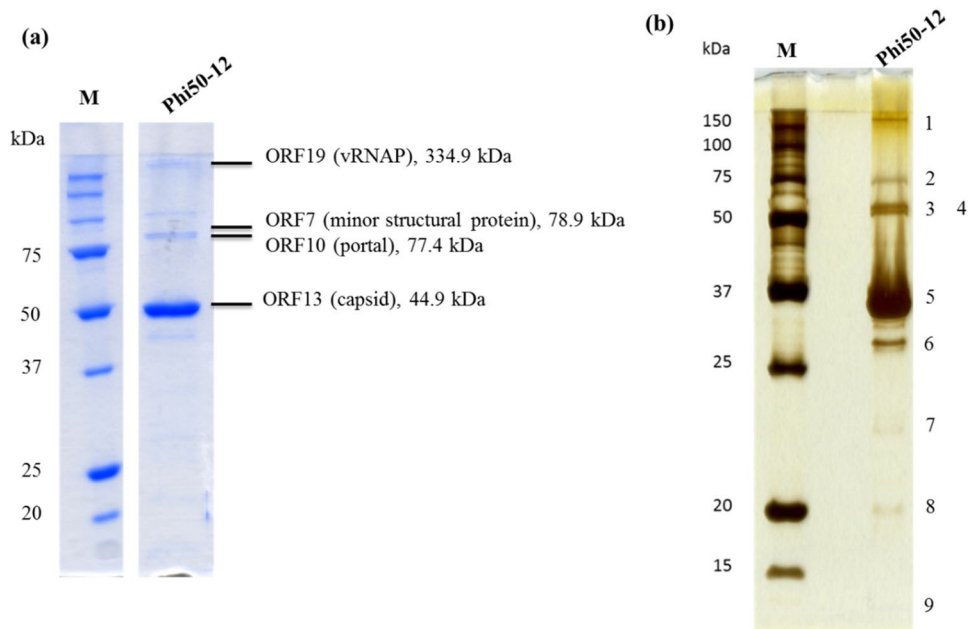


Figure 5. Structural protein analysis by 12% SDS-PAGE. **(a)** Phage particles (5×10^{11} PFU) were boiled in protein sample buffer (80 mM Tris, pH 6.8; 2% SDS; 2-mercaptoethanol; 0.0006% Bromophenol blue) and subjected to SDS-PAGE. Parallely, the sliced bands were subjected to LC/MS/MS analysis. Peptides matched with the annotated ORFs, and their observed molecular mass were indicated. Four of them were identified to be virion-encapsulated RNA polymerase (ORF19), minor structural protein (ORF7), portal protein (ORF10) and capsid protein (ORF13), respectively. Original gel is presented in Supplementary Fig. S9. **(b)** For better visualization, a silver stain procedure was also performed, nine bands were visible on the gel. Numbers indicate the protein band location. M is the molecular weight marker, phi50-12 represents the structural protein lysate.

family comprises 8 subfamilies and 22 new genera. To determine the phylogenetic relationship between phi50-12 and other N4-like phages, we chose terminase (Fig. 7a), vRNAP (Supplementary Fig. S8), and DNA polymerase (DNAP) (Supplementary Fig. S8) as candidates to collect the corresponding sequences from the available orthologous sequences of N4-like phages and performed phylogenetic analysis. The results demonstrated that phi50-12 was present as a single branch, which now has been placed under genus *Penintadodekavirus* as species *penintadodekavirus* 5012, but shared the same group as smaller N4-like vibrio phages. The most closely related genome was that of pVco5, a phage that infects *Vibrio coralliilyticus* and belongs to a new genus *Vicoquintavirus*. All three genes showed a similar tree patterns. We also performed a genome-wide comparison with all vibrio phages using VIPTree⁴⁵. The proteomic tree demonstrated similar results in a single gene tree (Fig. 7b); phi50-12 clustered with N4-like vibrio phages and formed a single branch, but was close to the genomes of N4 vibrio phages. This may indicate that the intertidal zone is a specific microenvironment for the evolution of the unique features of phi50-12.

Assessment of bacterial growth inhibition of phi50-12 in zebrafish. The application of phage therapy instead of antibiotics to eliminate pathogenic bacteria in *Vibrio* to reduce fish mortality in aquaculture has been previously reported^{46–48}. Thus, the reduced bacterial growth by phi50-12 increased the survival of zebrafish was measured using the cumulative mortality over 10 days. The efficacy to reduce the mortality of fish with phi50-12 was measured after challenge with GRA50-12 for 30 min, followed by injection with phi50-12 at MOI = 10. Compared to the GRA50-12 challenged group, phi50-12 administration significantly reduced cumulative mortality within 3 days (41.6% vs. 87.5%). After 10 days, only four zebrafish died when treated with phi50-12, whereas 17 died in the GRA50-12 challenged group. Fish injected with phi50-12, or with PB3S buffer only, remained alive until the end of the experiment (Fig. 8a). The disease symptoms of GRA50-12 infected zebrafish were monitored; whereas PB3S buffer and phi50-12 injected groups showed no disease symptoms (Fig. 8b, Control/PB3S). The zebrafish injected with GRA50-12 in the absence or presence of phi50-12 showed a swollen abdomen and bleeding on the body surface (Figs. 1b and 8b, MOI = 10), but the symptoms were mild in the phi50-12 rescued group. This suggests that phi50-12 administration can cease the symptoms of diseased fish successfully, in most cases. The anatomy of diseased fish in the phi50-12 rescued group also showed swollen and bleeding intestines. One fish died on the 10th day in the phi50-12 only group, which was assumed to be a natural death.

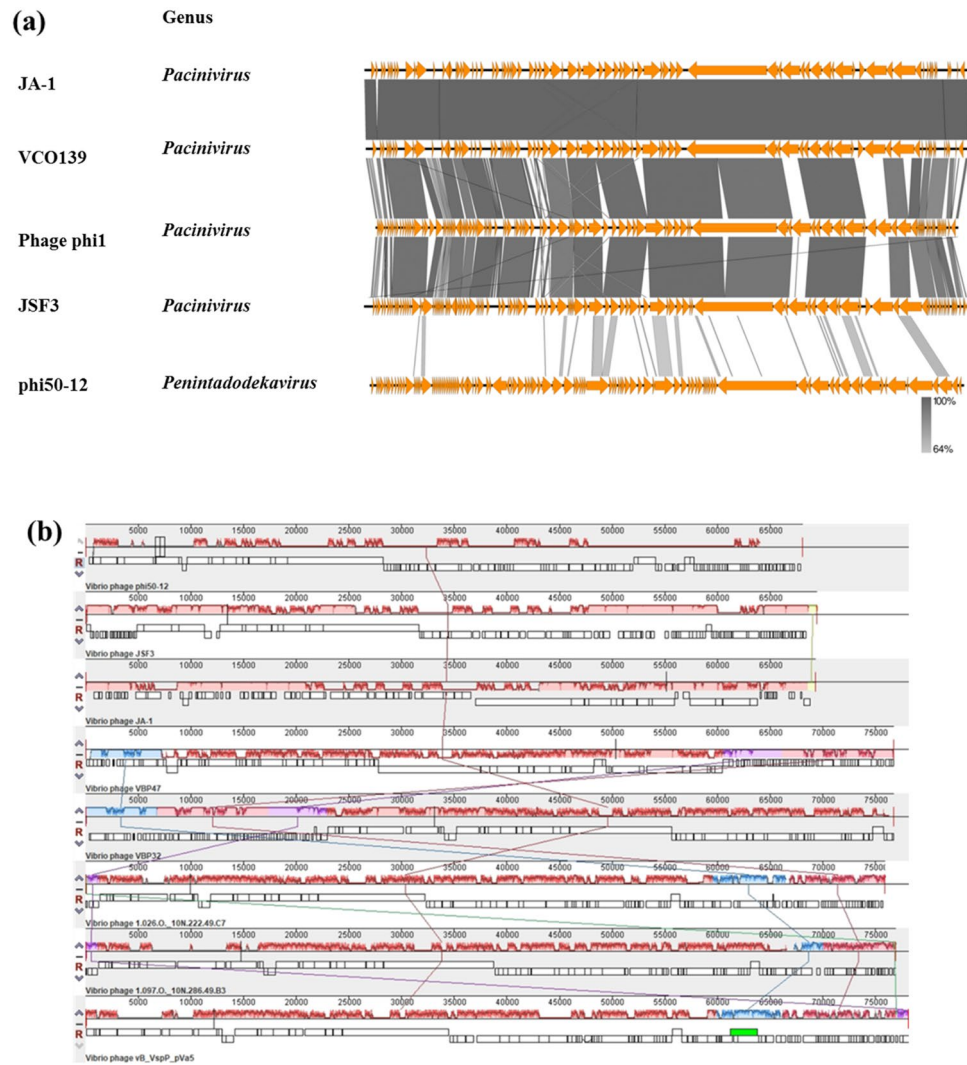


Figure 6. Comparative genomic analysis of N4-like *Vibrio* phages. **(a)** TBLASTX was performed by Easyfig. All the phages belong to N4-like *Vibrio* phages. “Genus” represents the taxonomy to which they belong. The similarity range is indicated by the gradient scale. **(b)** Mauve alignment of selected N4-like *Vibrio* phages infecting a variety of *Vibrio* hosts. The hosts include *V. owensii* (phi50-12), *V. cholera* (JSF3, JA-1), *V. parahaemolyticus* (VBP47, VBP32), unidentified hosts (*Vibrio* phage 1.026.O_10N222.49.C7, 1.097.O_10N.286.49.B3), *Vibrio splendidus* (vB_VspP_pVa5). Each colored block represents a region of collinear sequence (LCB, local collinear block) among genomes. White boxes represent the ORFs of each genome and their arrangements.

Conclusions

This study identified the coral symbiont *V. owensii* GRA50-12 as a potent pathogen using phenotypical, biochemical, and zebrafish toxicity tests. Many *Vibrio* species in the Harveyi clade are pathogenic to aquatic animals, especially to shrimp larvae, lobster, juvenile fish, shellfish, mollusks⁴⁹ and corals⁵⁰. This has negatively affected the economy of the aquaculture industry worldwide. A virulent phage belonging to the species *Schitoviridae* of the N4-like phage family⁴⁴ was isolated and characterized. The sequence showed novelty with no closely related sequences. Although, phi50-12 has a limited host range, it showed sensitivity to *Vibrio* spp. isolated from the same ecological niche. Phi50-12 has a short adsorption time, a large burst size, and stability over a wide range of pH and temperatures. In addition, in vitro and in vivo analyses showed that phi50-12 had a strong lytic ability against *V. owensii* GRA50-12. Complete genome and phylogenetic analysis of phi50-12 confirmed the absence of any antibiotic resistance genes or virulence factors. This study is the first to report the pathogenicity of localized *V. owensii* in Taiwan and its interaction with a newly isolated phage. The measurement of survival in the zebrafish model suggests that phi50-12 is a good candidate for reducing the population of *V. owensii*, which may be useful for the prevention and control of diseases caused by *V. owensii*. However, extensive studies must be carried out further so as to ascertain these therapeutic effects.

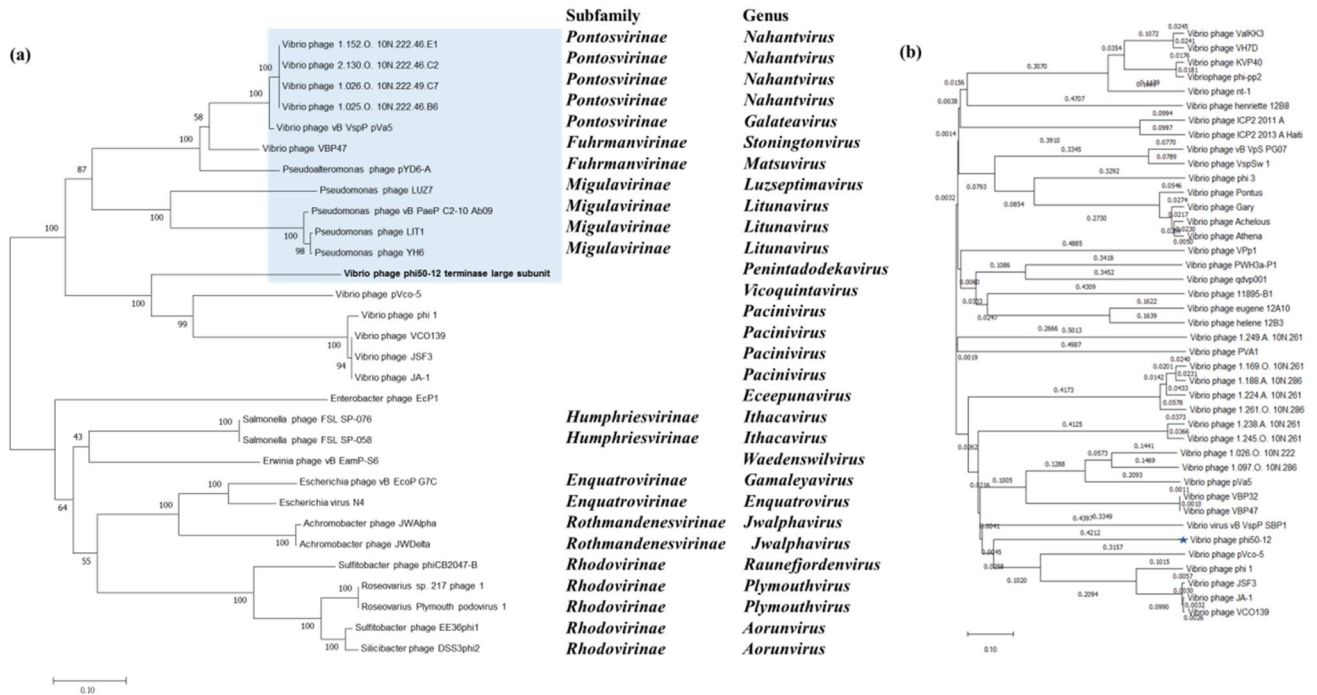


Figure 7. Phylogenetic analysis of terminase large subunit and viral proteomic tree analysis. **(a)** The tree generated by MEGA11 based on Neighbor-joining method with 1000 bootstraps. The subfamily and genus of the phages are indicated on the right. **(b)** Viral proteomic tree generated by VIPTree. This analysis involved all *Vibrio* phages available in the reference database at present.

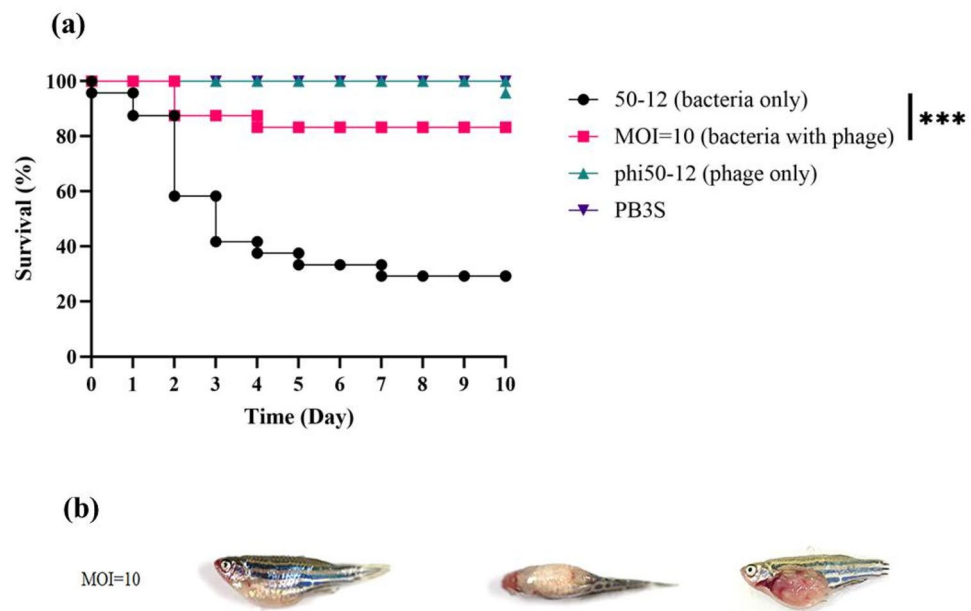


Figure 8. Therapeutic effect of phi50-12 in zebrafish. **(a)** Four groups were considered, each containing 24 fishes. These were subjected to four distinct conditions: injection with *V. owensii* GRA50-12 cells ($2.8\text{--}4.5 \times 10^6$ CFU/20 μl , black line), phi50-12 treatment (MOI=10) for 30 min followed by challenge with bacteria (red line), phi50-12 treatment only (green line) and PB3S buffer as negative control (purple line); and survival rates were measured. The X-axis represents the time post-infection and the Y-axis represents the survival percentage of the zebra fish. **(b)** The disease symptoms of zebrafish rescued by phi50-12 with MOI=10. *V. owensii* GRA50-12 introduced first in the fish followed by administration of phi50-12 after 30 min. MOI=10 represents the disease symptom of sick fish in the group with phi50-12 administration. Left: side view; middle: top view; right: abdomen anatomy. The anatomical picture showed swollen abdomen and bleeding intestines. The significance of the differences between groups was performed by Log-rank and Gehan–Breslow–Wilcoxon test in GraphPad Prism 9. “***” indicates $p < 0.001$.

Materials and methods

Conditions of cultivation. All *Vibrio* spp. used in this study are listed in Table 1, and most of them (except those where the sources are specified) were originally isolated from several kinds of macroalgae on corals in the intertidal zone of Shihti Fishing Port in the east of Hualien County. The water samples were provided by Dr. Chen CY (Department of Life Science, Tzu Chi University). Cultures were grown at 30 °C in TSB medium (BD-Difco, USA) with 3% of NaCl and aerated by shaking at 150 rpm. TSB3S containing 1.5% agar was used for routine plate cultures, whereas TSB3S containing 0.75% agar for the double agar overlay method was used for the spot test and titration of the phage in the plaque assay.

Phage isolation and purification. Phage phi50-12 was isolated from a water sample from the intertidal zone around the location where the host *V. owensii* GRA50-12 was isolated. The collected water sample was filtered through a 0.22 µm filter membrane. The filtered water sample (9.0 ml) was mixed with 50 µl of *V. owensii* GRA50-12 cells grown to log phase (2×10^8 CFU/ml). The mixtures were grown overnight to enrich for possible existing phages. Furthermore, 5 µl of the culture supernatant was spotted onto the bacterial lawns grown on soft agar (0.75%) using the double agar overlay method. The clearing zones formed on the lawns were subjected to three rounds of single plaque isolation. A single plaque on the lawn of GRA50-12 was picked and enriched thrice to obtain a pure phage population. High titer lysates of the phage (50 ml containing $\sim 10^{12}$ PFU/ml) were concentrated, centrifuged at 46,500g (Beckman Coulter Avanti centrifuge, J25I rotor; Beckman Coulter, Brea, CA, USA) for 3 h at 4 °C. The pellets were suspended in 1.0 ml SM buffer (0.05 M Tris-HCl, pH 7.5, 0.1 M NaCl, 0.008 M MgSO₄·7H₂O, and 0.01% gelatin) and loaded onto block gradients of CsCl (1.3, 1.4, 1.45, 1.5, 1.6 and 1.7 g/ml), followed by ultracentrifugation (154,000g for 3 h at 4 °C with an SW41Ti rotor in an Optima LE-80K Ultracentrifuge from Beckman Coulter). The phage particles were recovered from the gradient and desalted by dialysis.

Phage DNA isolation and pulsed-field gel electrophoresis. We followed the procedures described by Chang et al.⁵¹ to isolate phage DNA and perform restriction enzyme digestion. PFGE was performed as previously described⁵², and the CHEF-DR III System (Bio-Rad Laboratories, Hercules, CA, USA) was used under the following conditions: 9 °C in 0.5× Tris-borate-EDTA buffer (pH 8.0) at 6 V/cm with pulse ramps from 3.5 to 4 s for 19.5 h. A Midrange IPFG Marker (New England Biolabs, Ipswich, MA, USA) was used as the molecular size standard.

Genome analysis. The genomic sequence of phi50-12 was determined by the Genomics Company, Taiwan. The average genome coverage is (approximately) 2729×.

Genome annotation was performed using Glimmer⁵³ and GeneMark⁵⁴. We also referred to InteroProScan (<https://www.ebi.ac.uk/interpro/search/sequence/>) and HHpred (<https://toolkit.tuebingen.mpg.de/tools/hhpred>) as tools to obtain best possible annotation for phage phi50-12. Functional predictions were made using BLASTP. Potential tRNA and tmRNA genes were predicted by Aragorn et al.³⁵ and tRNAScanSE³⁶. Antibiotic genes and virulence factors were identified using ResFinder and VirulenceFinder³⁶. Phylogenetic analysis was performed using MEGA 11 software⁵⁵. Comparative genomic analysis was performed using Easyfig 2.2.3⁵⁶ and Mauve alignment⁵⁷.

Transmission electron microscopy. Purified phage particles were applied to the surface of a formvar-coated grid, negatively stained with 1% phosphotungstic acid (PTA), and then examined by TEM (Hitachi Company, Japan).

Determination of the phage adsorption and growth curve. Phage adsorption curve was determined by growing host cells to log phase ($\sim 2 \times 10^8$ /ml after 1.5 h subculturing), then infected with phi50-12 at an MOI of 0.0005, and incubated at 30 °C. Aliquots of 500 µl were taken at an interval of every 3 min and centrifuged (12,000×g, 5 min). 100 µl of supernatant was removed to calculate the titer of unadsorbed phages. One-step growth and burst-size measurements were performed as previously reported⁵⁸. All experiments were performed at least twice in triplicates.

Stability to physical, chemical and environmental factors. Except for UV radiation treatment (10^3 PFU/ml), a phage suspension of concentration 4×10^6 PFU/ml was used for all individual treatments. For temperature sensitivity tests, phage suspensions were incubated at different temperatures for 24 h. Salinity tests were carried out by incubating phage suspensions in different percentages of NaCl-containing media for 24 h. To simulate phage exposure under UV radiation in a natural environment, phage suspensions were diluted to 10^3 PFU/ml and exposed to UV-C radiation for 15 min and 24 h. The loss of infectivity was measured using the plaque-forming assay method.

Structural proteins analysis. The phage particles were purified using CsCl and concentrated. The suspension was mixed with protein sample buffer, boiled for 10 min, and then separated on a 12% SDS-PAGE gel. Protein size markers were purchased from Bio-Rad, and the protein bands were visualized using InstantBlue (Expedeon Protein Solutions, Ltd., Cambridge, UK). For better visualization of low-copy structural proteins, gels were stained using the silver staining method⁵⁹. The identity of the virion proteins was elucidated using LC/MS/MS (Energensis Biomedical Co., Ltd., Taiwan).

In vitro lysis. Mid-log phase cells were loaded into 96-well microplate and mixed with different MOIs of phi50-12 in 200 µl medium in triplicate. The plates were incubated at 30 °C. At each time point, the optical density of the plate was measured at a wavelength of 600 nm (Thermo Scientific Varioskan Flash). Three wells that were not loaded with phi50-12 served as the controls. The cell lysis curve was monitored every 30 min for 10 h.

Host range analysis. The host range was determined by spotting 5 µl of phage lysate on the lawns of investigated cultures on TSB3S agar plates, as previously described⁵⁸. A clear spot indicates host sensitivity.

Zebrafish infections. The zebrafish (*Danio rerio*) lines used in this study were the wild type AB variety which were maintained and grown in the Tzu Chi University FishCore facility according to standard protocols. All protocols in accordance with the guidelines and regulations of council of Agriculture Executive Yuan (Taiwan) for the care and use of laboratory animals. Mixed male and female populations of zebrafish were kept in 9 L tanks at 28 °C and maintained in a 14 h light/10 h dark cycle. All methods used in this study were performed in accordance with the guidelines and regulations of Institutional Animal Care and Use Committee (IACUC) in Tzu-Chi University.

For confirmation of pathogenicity of GRA50-12, a total of 24 adult male and female fish (approximately 3–3.5 cm) were mixed and divided into three groups (8 fishes/ group). Two different bacterial cell counts (2.2×10^6 CFU/20 µl and 2.2×10^4 CFU/20 µl) were applied and one used PB3S as control. Before injection, individuals anesthetized with 160 mg/ml tricaine then were injected intraperitoneally with insulin needle.

For the measurement of reduced bacterial growth by phi50-12, mixed adult male and female fish were grouped into 24 fishes per group. One group was injected with 20 µl ($2.8\text{--}4.5 \times 10^7$ CFU) of *V. owensii* GRA50-12 suspended in PB3S through the cloaca with an insulin needle. The other group was infected with the same dose of *V. owensii* GRA50-12 and injected 30 min later with a dose of phi50-12 (MOI = 10 in 20 µl) into the cloaca. phi50-12 treatment only and PB3S buffer as negative control. The significance of the differences between groups was determined using the Log-rank and Gehan–Breslow–Wilcoxon test in GraphPad Prism 9.

Zebrafish use was performed in agreement with ARRIVE guidelines (<https://arriveguidelines.org>). The laboratory protocol was approved by the Institutional Animal Care and Use Committee of Tzu Chi University (IACUC approval no. 109018).

Nucleotide sequence accession number. The genome sequence of phi50-12 was deposited in GenBank under accession number MN584918.1.

Institutional Review Board statement. The laboratory protocol was approved by the Institutional Animal Care and Use Committee of Tzu Chi University (IACUC Approval No.: 109018).

Data availability

The data presented in this study are available in this article and supplementary material here.

Received: 29 July 2022; Accepted: 19 September 2022

Published online: 30 September 2022

References

- Thompson, F. L., Iida, T. & Swings, J. Biodiversity of vibrios. *Microbiol. Mol. Biol. Rev.* **68**, 403–431. <https://doi.org/10.1128/MMBR.68.3.403-431.2004> (2004) (table of contents).
- Poli, A. *et al.* *Vibrio coralliirubri* sp. Nov., a new species isolated from mucus of red coral (*Corallium rubrum*) collected at Procida island, Italy. *Antonie Van Leeuwenhoek* **111**, 1105–1115. <https://doi.org/10.1007/s10482-017-1013-5> (2018).
- Romalde, J. L., Dieguez, A. L., Lasa, A. & Balboa, S. New *Vibrio* species associated to molluscan microbiota: A review. *Front. Microbiol.* **4**, 413. <https://doi.org/10.3389/fmicb.2013.00413> (2014).
- Culot, A. *et al.* Isolation of Harveyi clade *Vibrio* spp. collected in aquaculture farms: How can the identification issue be addressed?. *J. Microbiol. Methods* **180**, 106106. <https://doi.org/10.1016/j.mimet.2020.106106> (2021).
- Yoshizawa, S. *et al.* *Vibrio jasicida* sp. Nov., a member of the Harveyi clade, isolated from marine animals (packhorse lobster, abalone and Atlantic salmon). *Int. J. Syst. Evol. Microbiol.* **62**, 1864–1870. <https://doi.org/10.1099/ijs.0.025916-0> (2012).
- Ruwandeeepika, H. A. *et al.* In vitro and in vivo expression of virulence genes in *Vibrio* isolates belonging to the Harveyi clade in relation to their virulence towards gnotobiotic brine shrimp (*Artemia franciscana*). *Environ. Microbiol.* **13**, 506–517. <https://doi.org/10.1111/j.1462-2920.2010.02354.x> (2011).
- Ushijima, B. *et al.* Disease diagnostics and potential coinfections by *Vibrio coralliilyticus* during an ongoing coral disease outbreak in Florida. *Front. Microbiol.* **11**, 569354. <https://doi.org/10.3389/fmicb.2020.569354> (2020).
- Ushijima, B., Smith, A., Aeby, G. S. & Callahan, S. M. *Vibrio owensii* induces the tissue loss disease Montipora white syndrome in the Hawaiian reef coral *Montipora capitata*. *PLoS One* **7**, e46717. <https://doi.org/10.1371/journal.pone.0046717> (2012).
- Defoirdt, T., Boon, N., Sorgeloos, P., Verstraete, W. & Bossier, P. Quorum sensing and quorum quenching in *Vibrio harveyi*: Lessons learned from in vivo work. *ISME J.* **2**, 19–26. <https://doi.org/10.1038/ismej.2007.92> (2008).
- Ke, H. M. *et al.* Comparative genomics of *Vibrio campbellii* strains and core species of the *Vibrio* Harveyi clade. *Sci. Rep.* **7**, 41394. <https://doi.org/10.1038/srep41394> (2017).
- Hoffmann, M., Monday, S. R., Fischer, M. & Brown, E. W. Genetic and phylogenetic evidence for misidentification of *Vibrio* species within the Harveyi clade. *Lett. Appl. Microbiol.* **54**, 160–165. <https://doi.org/10.1111/j.1472-765X.2011.03183.x> (2012).
- Ke, H. M. *et al.* Tracing genomic divergence of vibrio bacteria in the Harveyi clade. *J. Bacteriol.* <https://doi.org/10.1128/JB.00001-18> (2018).
- Cano-Gomez, A., Goulden, E. F., Owens, L. & Hoj, L. *Vibrio owensii* sp. nov., isolated from cultured crustaceans in Australia. *FEMS Microbiol. Lett.* **302**, 175–181. <https://doi.org/10.1111/j.1574-6968.2009.01850.x> (2010).
- Goulden, E. F., Hall, M. R., Bourne, D. G., Pereg, L. L. & Hoj, L. Pathogenicity and infection cycle of *Vibrio owensii* in larviculture of the ornate spiny lobster (*Panulirus ornatus*). *Appl. Environ. Microbiol.* **78**, 2841–2849. <https://doi.org/10.1128/AEM.07274-11> (2012).

15. Liu, L. *et al.* A *Vibrio owensii* strain as the causative agent of AHPND in cultured shrimp, *Litopenaeus vannamei*. *J. Invertebr. Pathol.* **153**, 156–164. <https://doi.org/10.1016/j.jip.2018.02.005> (2018).
16. Liang, X., Zhou, L., Yan, S. & Wang, Y. Complete genome sequence analysis of the *Vibrio owensii* strain SH-14 isolated from shrimp with acute hepatopancreatic necrosis disease. *Arch. Microbiol.* **202**, 1097–1106. <https://doi.org/10.1007/s00203-020-01824-z> (2020).
17. Liu, L. *et al.* Draft genome sequence of *Vibrio owensii* strain SH-14, which causes shrimp acute hepatopancreatic necrosis disease. *Genome Announc.* <https://doi.org/10.1128/genomeA.01395-15> (2015).
18. Wang, J. T., Chu, C. W. & Soong, K. Comparison of the bleaching susceptibility of coral species by using minimal samples of live corals. *PeerJ* **10**, e12840. <https://doi.org/10.7717/peerj.12840> (2022).
19. Lazar, V. *et al.* Antibiotic resistance profiles in cultivable microbiota isolated from some Romanian natural fishery lakes included in Natura 2000 network. *BMC Vet. Res.* **17**, 52. <https://doi.org/10.1186/s12917-021-02770-8> (2021).
20. Soliman, W. S., Shaapan, R. M., Mohamed, L. A. & Gayed, S. S. R. Recent biocontrol measures for fish bacterial diseases, in particular to probiotics, bio-encapsulated vaccines, and phage therapy. *Open Vet. J.* **9**, 190–195. <https://doi.org/10.4314/ovj.v9i3.2> (2019).
21. Yu, Y. P. *et al.* Isolation and characterization of five lytic bacteriophages infecting a *Vibrio* strain closely related to *Vibrio owensii*. *FEMS Microbiol. Lett.* **348**, 112–119. <https://doi.org/10.1111/1574-6968.12277> (2013).
22. Lin, L. C., Lin, G. H., Tseng, Y. H. & Yu, M. S. Draft genome sequence of *Vibrio owensii* GRA50-12, isolated from green algae in the intertidal zone of Eastern Taiwan. *Genome Announc.* <https://doi.org/10.1128/genomeA.01438-14> (2015).
23. Urbanczyk, H., Ogura, Y. & Hayashi, T. Contrasting inter- and intraspecies recombination patterns in the “Harveyi clade” vibrio collected over large spatial and temporal scales. *Genome Biol. Evol.* **7**, 71–80. <https://doi.org/10.1093/gbe/evu269> (2014).
24. Babbitt, A. R. *et al.* Discovery and quantification of anaerobic nitrogen metabolisms among oxygenated tropical Cuban stony corals. *ISME J.* **15**, 1222–1235. <https://doi.org/10.1038/s41396-020-00845-2> (2021).
25. Li, H. *et al.* *Vibrio alginolyticus* 16S–23S intergenic spacer region analysis, and PCR assay for identification of coral pathogenic strain XSBZ03. *Dis. Aquat. Organ.* **129**, 71–83. <https://doi.org/10.3354/dao03233> (2018).
26. Chun, D., Chung, J. K., Tak, R. & Seol, S. Y. Nature of the Kanagawa phenomenon of *Vibrio parahaemolyticus*. *Infect. Immun.* **12**, 81–87. <https://doi.org/10.1128/iai.12.1.81-87.1975> (1975).
27. Nag, D., Farr, D. A., Walton, M. G. & Withey, J. H. Zebrafish models for pathogenic vibrios. *J. Bacteriol.* <https://doi.org/10.1128/JB.00165-20> (2020).
28. Knecht, L. E., Veljkovic, M. & Fieseler, L. Diversity and function of phage encoded depolymerases. *Front. Microbiol.* **10**, 2949. <https://doi.org/10.3389/fmicb.2019.02949> (2019).
29. McCarter, L. L. OpaR, a homolog of *Vibrio harveyi* LuxR, controls opacity of *Vibrio parahaemolyticus*. *J. Bacteriol.* **180**, 3166–3173. <https://doi.org/10.1128/JB.180.12.3166-3173.1998> (1998).
30. Huang, X. *et al.* Identification and characterization of a locus putatively involved in colanic acid biosynthesis in *Vibrio alginolyticus* ZJ-51. *Biofouling* **34**, 1–14. <https://doi.org/10.1080/08927014.2017.1400020> (2018).
31. Johnson, J. A., Panigrahi, P. & Morris, J. G. Jr. Non-O1 *Vibrio cholerae* NRT36S produces a polysaccharide capsule that determines colony morphology, serum resistance, and virulence in mice. *Infect. Immun.* **60**, 864–869. <https://doi.org/10.1128/iai.60.3.864-869.1992> (1992).
32. Yoshida, S., Ogawa, M. & Mizuguchi, Y. Relation of capsular materials and colony opacity to virulence of *Vibrio vulnificus*. *Infect. Immun.* **47**, 446–451. <https://doi.org/10.1128/iai.47.2.446-451.1985> (1985).
33. Shkoporov, A. N. *et al.* Long-term persistence of crAss-like phage crAss001 is associated with phase variation in *Bacteroides intestinalis*. *BMC Biol.* **19**, 1–163. <https://doi.org/10.1186/s12915-021-01084-3> (2021).
34. Fouts, D. E. *et al.* Whole genome sequencing and comparative genomic analyses of two *Vibrio cholerae* O139 Bengal-specific Podoviruses to other N4-like phages reveal extensive genetic diversity. *Virol. J.* **10**, 165. <https://doi.org/10.1186/1743-422X-10-165> (2013).
35. Laslett, D. & Canback, B. ARAGORN, a program to detect tRNA genes and tmRNA genes in nucleotide sequences. *Nucleic Acids Res.* **32**, 11–16. <https://doi.org/10.1093/nar/gkh152> (2004).
36. Chan, P. P. & Lowe, T. M. tRNAscan-SE: Searching for tRNA genes in genomic sequences. *Methods Mol. Biol.* **1962**, 1–14. https://doi.org/10.1007/978-1-4939-9173-0_1 (2019).
37. Kleinheinz, K. A., Joensen, K. G. & Larsen, M. V. Applying the ResFinder and VirulenceFinder web-services for easy identification of acquired antibiotic resistance and *E. coli* virulence genes in bacteriophage and prophage nucleotide sequences. *Bacteriophage* **4**, e27943. <https://doi.org/10.4161/bact.27943> (2014).
38. Davydova, E. K., Santangelo, T. J. & Rothman-Denes, L. B. Bacteriophage N4 virion RNA polymerase interaction with its promoter DNA hairpin. *Proc. Natl. Acad. Sci. U.S.A.* **104**, 7033–7038. <https://doi.org/10.1073/pnas.0610627104> (2007).
39. Willis, S. H., Kazmierczak, K. M., Carter, R. H. & Rothman-Denes, L. B. N4 RNA polymerase II, a heterodimeric RNA polymerase with homology to the single-subunit family of RNA polymerases. *J. Bacteriol.* **184**, 4952–4961. <https://doi.org/10.1128/JB.184.18.4952-4961.2002> (2002).
40. Wittmann, J. *et al.* Taxonomic reassessment of N4-like viruses using comparative genomics and proteomics suggests a new subfamily—“Enquartavirinae”. *Arch. Virol.* **160**, 3053–3062. <https://doi.org/10.1007/s00705-015-2609-6> (2015).
41. Paddison, P. *et al.* The roles of the bacteriophage T4 r genes in lysis inhibition and fine-structure genetics: A new perspective. *Genetics* **148**, 1539–1550. <https://doi.org/10.1093/genetics/148.4.1539> (1998).
42. Schito, G. C. Development of coliphage N4: Ultrastructural studies. *J. Virol.* **13**, 186–196. <https://doi.org/10.1128/JVI.13.1.186-196.1974> (1974).
43. Ma, Y. *et al.* Isolation and molecular characterisation of Achromobacter phage phiAxp-3, an N4-like bacteriophage. *Sci. Rep.* **6**, 24776. <https://doi.org/10.1038/srep24776> (2016).
44. Wittmann, J. *et al.* From orphan phage to a proposed new family—the diversity of N4-like viruses. *Antibiotics (Basel)*. <https://doi.org/10.3390/antibiotics9100663> (2020).
45. Nishimura, Y. *et al.* ViPTree: The viral proteomic tree server. *Bioinformatics* **33**, 2379–2380. <https://doi.org/10.1093/bioinformatics/btx157> (2017).
46. Cerveny, K. E., DePaola, A., Duckworth, D. H. & Gulig, P. A. Phage therapy of local and systemic disease caused by *Vibrio vulnificus* in iron-dextran-treated mice. *Infect. Immun.* **70**, 6251–6262. <https://doi.org/10.1128/IAI.70.11.6251-6262.2002> (2002).
47. Gao, L. *et al.* Isolation and characterization of a lytic vibriophage OY1 and its biocontrol effects against *Vibrio* spp. *Front. Microbiol.* **13**, 830692. <https://doi.org/10.3389/fmicb.2022.830692> (2022).
48. Kalatzis, P. G., Bastias, R., Kokkari, C. & Katharios, P. Isolation and characterization of two lytic bacteriophages, phiSt2 and phiGrn1; phage therapy application for biological control of *Vibrio alginolyticus* in aquaculture live feeds. *PLoS One* **11**, e0151101. <https://doi.org/10.1371/journal.pone.0151101> (2016).
49. de Souza Valente, C. & Wan, A. H. L. *Vibrio* and major commercially important vibriosis diseases in decapod crustaceans. *J. Invertebr. Pathol.* **181**, 107527. <https://doi.org/10.1016/j.jip.2020.107527> (2021).
50. Weynberg, K. D., Woolstra, C. R., Neave, M. J., Buerger, P. & van Oppen, M. J. From cholera to corals: Viruses as drivers of virulence in a major coral bacterial pathogen. *Sci. Rep.* **5**, 17889. <https://doi.org/10.1038/srep17889> (2015).
51. Chang, H. C. *et al.* Isolation and characterization of novel giant *Stenotrophomonas maltophilia* phage phiSMA5. *Appl. Environ. Microbiol.* **71**, 1387–1393. <https://doi.org/10.1128/AEM.71.3.1387-1393.2005> (2005).

52. Tseng, Y. H. *et al.* Chromosome map of *Xanthomonas campestris* pv. *campestris* 17 with locations of genes involved in xanthan gum synthesis and yellow pigmentation. *J. Bacteriol.* **181**, 117–125. <https://doi.org/10.1128/JB.181.1.117-125.1999> (1999).
53. Delcher, A. L., Harmon, D., Kasif, S., White, O. & Salzberg, S. L. Improved microbial gene identification with GLIMMER. *Nucleic Acids Res.* **27**, 4636–4641. <https://doi.org/10.1093/nar/27.23.4636> (1999).
54. Lukashin, A. V. & Borodovsky, M. GeneMark.hmm: New solutions for gene finding. *Nucleic Acids Res.* **26**, 1107–1115. <https://doi.org/10.1093/nar/26.4.1107> (1998).
55. Kumar, S., Tamura, K. & Nei, M. MEGA: Molecular evolutionary genetics analysis software for microcomputers. *Comput. Appl. Biosci.* **10**, 189–191. <https://doi.org/10.1093/bioinformatics/10.2.189> (1994).
56. Sullivan, M. J., Petty, N. K. & Beatson, S. A. Easyfig: A genome comparison visualizer. *Bioinformatics* **27**, 1009–1010. <https://doi.org/10.1093/bioinformatics/btr039> (2011).
57. Darling, A. C., Mau, B., Blattner, F. R. & Perna, N. T. Mauve: Multiple alignment of conserved genomic sequence with rearrangements. *Genome Res.* **14**, 1394–1403. <https://doi.org/10.1101/gr.2289704> (2004).
58. Wang, J. B., Yu, M. S., Tseng, T. T. & Lin, L. C. Molecular characterization of Ahp2, a lytic bacteriophage of *Aeromonas hydrophila*. *Viruses* <https://doi.org/10.3390/v13030477> (2021).
59. Kumar, G. Principle and method of silver staining of proteins separated by sodium dodecyl sulfate-polyacrylamide gel electrophoresis. *Methods Mol. Biol.* **1853**, 231–236. https://doi.org/10.1007/978-1-4939-8745-0_26 (2018).
60. Urbanczyk, Y., Ogura, Y., Hayashi, T. & Urbanczyk, H. Description of a novel marine bacterium *Vibrio hyugaensis* sp. nov., based on genomic and phenotypic characterization. *Syst Appl Microbiol* **38**, 300–304. <https://doi.org/10.1016/j.syapm.2015.04.001> (2015).
61. Yoshizawa, S. *et al.* *Vibrio jasicida* sp. nov., a member of the Harveyi clade, isolated from marine animals (packhorse lobster, abalone and Atlantic salmon). *Int J Syst Evol Microbiol* **62**, 1864–1870. <https://doi.org/10.1099/ijs.0.025916-0> (2012).

Acknowledgements

We thank the Electron Microscopy Laboratory of Tzu Chi University for their technical assistance.

Author contributions

Conceptualization, L.-C.L., Y.-C.T.; methodology, L.-C.L.; software, L.-C.L., Y.-C.T.; validation, L.-C.L., Y.-C.T.; formal analysis, L.-C.L.; resources, L.-C.L.; data curation, L.-C.L., Y.-C.T.; writing—original draft preparation, L.-C.L.; writing—review and editing, L.-C.L.; visualization, L.-C.L., Y.-C.T.; supervision, L.-C.L.; project administration, L.-C.L.; funding acquisition, L.-C.L. All authors have read and agreed to the published version of the manuscript.

Funding

This research was funded by grants TCIRP 98003-01 from Tzu Chi University and MOST 107-2635-B-320-003 from the Ministry of Sciences and Technology of Taiwan.

Competing interests

The authors declare no competing interests.

Additional information

Supplementary Information The online version contains supplementary material available at <https://doi.org/10.1038/s41598-022-20831-2>.

Correspondence and requests for materials should be addressed to L.-C.L.

Reprints and permissions information is available at www.nature.com/reprints.

Publisher's note Springer Nature remains neutral with regard to jurisdictional claims in published maps and institutional affiliations.



Open Access This article is licensed under a Creative Commons Attribution 4.0 International License, which permits use, sharing, adaptation, distribution and reproduction in any medium or format, as long as you give appropriate credit to the original author(s) and the source, provide a link to the Creative Commons licence, and indicate if changes were made. The images or other third party material in this article are included in the article's Creative Commons licence, unless indicated otherwise in a credit line to the material. If material is not included in the article's Creative Commons licence and your intended use is not permitted by statutory regulation or exceeds the permitted use, you will need to obtain permission directly from the copyright holder. To view a copy of this licence, visit <http://creativecommons.org/licenses/by/4.0/>.

© The Author(s) 2022